

Supporting Information for

Electronic supplementary information (ESI)

Bio-Inspired Antibacterial Cellulose Paper-Poly(amidoxime) Composite Hydrogel for High-Efficient Uranium(VI) Capture from Seawater

*Jinxiang Gao,^a Yihui Yuan,^a Qiuhan Yu,^a Bingjie Yan,^a Yongxin Qian,^a Jun Wen,^c Chunxin Ma,^{*a} Shaohua Jiang,^b Xiaolin Wang,^c Ning Wang^{*a}*

- a. State Key Laboratory of Marine Resource Utilization in South China Sea, Hainan University, Haikou 570228, P. R. China

E-mail: wangn02@foxmail.com, machunxin@hainanu.edu.cn

- b. Materials Science and Engineering, Nanjing Forestry University,

Nanjing 210037, P. R. China

- c. Institute of Nuclear Physics and Chemistry, China Academy of Engineering Physics,

Mianyang 621900, P. R. China

Table of contents

| | |
|--|----|
| Experimental section | 3 |
| Materials..... | 3 |
| Characterizations..... | 3 |
| Synthesis of poly(amidoxime) (PAO)..... | 4 |
| Fabrication of the antibacterial cellulose paper-poly(amidoxime) composite hydrogel..... | 4 |
| Test of the antibacterial performance..... | 5 |
| Calculation of the uranium-uptake capacity..... | 5 |
| Test of the uranium adsorption selectivity of the hydrogel..... | 6 |
| Method of the uranium desorption performance | 6 |
| Method of the uranium Extraction from the natural seawater..... | 6 |
| Data analysis | 7 |
| Figure S1 The curvilinear regression of uranium concentration-absorbance in uranium-spiked ultrapure water. | 7 |
| Figure S2 The curvilinear regression of uranium concentration-absorbance in uranium-spiked natural seawater. | 7 |
| Figure S3 (a) Synthesis of neutral PAO; (b) Transformation from water-insoluble PAO to water-soluble PAO containing negative charges. | 8 |
| Figure S4 The FT-IR spectra of PAN, PAO and cellulose-PAO hydrogel. | 8 |
| Figure S5 The ¹³ C-NMR spectra of (a) PAN and (b) PAO in DMSO-d ₆ , respectively. | 9 |
| Figure S6 Fabricating process of the primary cellulose-PAO composite hydrogel. | 10 |
| Figure S7 Cellulase enzymatic hydrolysis of the cellulose fiber. | 10 |
| Figure S8 Microscopic photos of composite hydrogel with different hydrolysis time. | 11 |
| Figure S9 Illustration to detect the contact angle of the (a) PAO and (b) the Cellulose-PAO composite hydrogel. | 11 |
| Figure S10 The contact angle of the cellulose-based napkin paper. | 12 |
| Figure S11 Uranium uptake capacity of composite hydrogel with different hydrolysis time in 16 ppm U-spiked filtered seawater. | 12 |
| Figure S12 Hydrogel weight and enzymatic hydrolysis rate during enzymatic hydrolysis. | 13 |
| Figure S13 The tensile strengths of composite hydrogels with different enzymatic hydrolysis rate. | 13 |
| Figure S14 Comparison of the C, O, U EDS mappings between the (a-f) U-uptake hydrogel and the (e-f) original Cellulose-PAO composite hydrogel. | 14 |
| Figure S15 Adsorption selectivity of the CP-PAO hydrogel for uranyl ions in simulated seawater. | 15 |
| Figure S16 pH dependence of the CP-PAO hydrogel for uranium adsorption in 8 ppm U-spiked pure water. | 15 |
| Figure S17 The uranium adsorption capacities and recovery rates of elution over 8 adsorption-desorption cycles. | 16 |
| Figure S18 Uranium desorption kinetics of the Napkin-PAO composite hydrogel in the elution solution. | 16 |
| Figure S19 The tensile stress of the antibacterial CP-PAO hydrogel before and after uranium elution over 8 adsorption-desorption cycles. | 17 |
| Figure S20 Comparison of uranium extraction between hydrogel substrate and Cellulose-PAO composite hydrogel. | 17 |
| Fig. S21 Comparison of the adsorption capacity of the CP-PAO hydrogel to the hydrogel-based and membrane-based adsorbents in U-spiked water and simulated seawater. | 18 |
| Figure S22 The seawater test system. (a) Plexiglass filter column. (b) Microfiltration membrane pump. (c) Seawater circulation device. (d) Seawater storage vessel. | 18 |
| Table S1 Concentration of U(VI) and co-existing metal ions in seawater and 100× seawater. | 19 |
| Table S2 Swelling ratio (SR) and water absorptivity (WA) of hydrogel. | 19 |
| Table S3 Mechanical properties of hydrogel and adsorption-desorption cycled hydrogels. | 20 |
| Supporting Movies | 20 |
| Movie S1 Preparation process of the Napkin-PAO composite hydrogel. | 20 |
| Movie S2 The Napkin-PAO composite hydrogel mechanical strength display. | 20 |
| Movie S3 U-adsorption process of the Napkin-PAO composite hydrogel in 100 ppm U-spiked water. | 20 |
| Movie S4 U-desorption process of the U-uptake Napkin-PAO composite hydrogel in elution solution. | 20 |
| References | 21 |

Experimental Section

Materials

Hydroxylamine hydrochloride ($\text{NH}_2\text{OH}\cdot\text{HCl}$, 99%), Polyacrylonitrile (PAN, 99%, average Mw 150,000), Dimethyl Diallyl Ammonium Chloride (DAC, 60%), N-Vinyl-2-pyrrolidone (NVP, 99%), 2,2'-azobis[2-methylpropionamide] dihydrochloride (AIBA), N,N'-Methylenebisacrylamide (BIS, 99%), N-Dimethylformamide (DMF, 99.9%), Arsenazo (III) (95%), Ammonium vanadate ($\text{NH}_4\text{VO}_3\cdot x\text{H}_2\text{O}$, 99.9%), Sodium hydroxide (NaOH, 99.5%), Cellulase and Zinc Chloride (ZnCl_2 , 98%) were phrased from Macklin. Sodium Chloride (NaCl, 99.0%), Ammonia ($\text{NH}_3\cdot\text{H}_2\text{O}$, 99.5%), Nickel Chloride hexahydrate ($\text{NiCl}_2\cdot 6\text{H}_2\text{O}$, 98%), Ferric Chloride hexahydrate ($\text{FeCl}_3\cdot 6\text{H}_2\text{O}$, 99%), Copper Sulfate pentahydrate ($\text{CuSO}_4\cdot 5\text{H}_2\text{O}$, 99%), $\text{C}_2\text{H}_5\text{OH}$ (99.5%) and Hydrochloric Acid (12 mol/L) were phrased from Xilong Scientific Co., Ltd. Cobalt Uranium hexahydrate Nitrate [$\text{UO}_2(\text{NO}_3)_2\cdot 6\text{H}_2\text{O}$, 99%]. Chloride hexahydrate ($\text{CoCl}_2\cdot 6\text{H}_2\text{O}$, 99%), was phrased from Chushengwei Chemical Co., Ltd. Napkin-paper was phrased from C&S Paper Co., Ltd. All the chemicals above were used as received without further purification. All the natural seawater was collected from the Chunyuan Sea nearby the Ganze Island in Wanning city of Hainan province in China and was used after filtered with a 0.45 μm filter membrane.

Characterization

Infrared (IR) data was collected on a Perkin-Elmer LR-64912C (FT-IR, LR 64912C, Perkin-Elmer, USA). Ultraviolet-visible (UV-Vis) absorption spectroscopy data was recorded on a AuCy spectrophotometer (UV1800PC, AuCy Instrument, China). X-ray photoelectron spectroscopy (XPS) spectra were performed on a Thermo ESCALAB 250XI and the binding energies were calibrated using the C1s peak at 284.82 eV (Thermo ESCALAB 250XI, Thermo Electron Corporation, U.S.A). ^{13}C NMR (Nuclear magnetic resonance) spectra was recorded on a Bruker Advance III 600M (NMR, Bruker AVANCE III 600M, Bruker, Germany). The hydrophilic property of the Napkin-paper/Poly(amidoxime) composite hydrogel was observed on a contact angle measuring instrument (JC2000D, Shanghai zhongchen digital technic apparatus CO., LTD, China). The microscope images were taken with a microscope (Olympus CX41RF, Japan). Scanning electron microscope (SEM) images were collected on a field emission scanning electron microscope (SEM, S-4800, HITACHI, Japan). The pH values were detected via a pH meter (F2, Mettler Toledo, Germany). Adsorption selectivity of the Napkin-PAO hydrogel on the uranyl ion and other metal ions in a simulated seawater was studied on inductively coupled plasma mass spectrometer (i-CAP RQ, Germany). The thickness of the hydrogel is measured by a spiral micrometer (US KNIGHT TOOL, Germany). The mechanical properties of the hydrogel membrane were detected through a tensile tester (GP-6113A, Germany).

Synthesis of the Poly(amidoxime) (PAO)

The Poly(amidoxime)(PAO) was synthesized based on the reported literature.^{1,2} $\text{NH}_2\text{OH}\cdot\text{HCl}$ (5.6 g, 80 mmol) was dissolved in DMF (60.0 mL) in a round-bottom flask heated by a water bath at 65 °C, Na_2CO_3 (3.06 g, 30 mmol) and NaOH (1.2 g, 30 mmol) was then added slowly; after stirring via a magnetic stirring apparatus for 3 hours, PAN (4.24 g, 80 mmol) was added and dissolved completely for at least 30 minutes, and then reacted at 65 °C for 24 hours. The reaction mixture was centrifuged and then the supernatant was dropped into 500 mL of ultra-pure water to precipitate a white floc. After filtering and gathering, the precipitate was dried within a vacuum at 55 °C for 12 h to obtain the as-prepared PAO.

Fabrication of the Antibacterial Cellulose Paper-Poly(amidoxime) composite hydrogel

The Antibacterial Napkin-PAO composite hydrogel was fabricated via a simple method. Firstly, the hydrogel precursor solution was prepared: the PAO (160 mg), the N-Vinyl-2-pyrrolidone monomer (30 mg) and the antibacterial monomer with the quaternary ammonium group (allyltrimethylammonium chloride, 10 mg), the crosslinker (N,N'-Methylenebisacrylamide, BIS, 6 mg) and the UV-initiator [(2,2'-azobis(2-methylpropionamide) dihydrochloride, AIBA, 6 mg] were dissolved in a 0.2 mol/L NaOH (3.0 mL). Secondly, the precursor solution was dropped slowly onto a napkin paper in the reactive tank and then was sealed with a piece of quartz glass sheet, after sitting for 10 min to let the precursor solution infiltrate into the napkin-paper enough, we can attain a preliminary Napkin-PAO hydrogel through UV-polymerization for 15 min (the intensity of the UV light: 2.5 ± 0.1 mW/cm²). Finally, the cellulose of the preliminary hydrogel was partly enzymolyzed to achieve the as-prepared Napkin-PAO composite hydrogel. Further, we performed enzymatic hydrolysis experiment on the the Napkin-PAO hydrogel, place 12 pieces of the Napkin-PAO hydrogel (dry weight is known) into the enzymatic hydrolysate containing cellulase. The enzymatic hydrolysis time was 3, 6, 9, 12, 15, 18, 21, 24, 27, 30, 33, 36 hours, respectively. After completion of the enzymatic hydrolysis, the hydrogel was taken out and placed in 0.01 mol/L NaOH aqueous solution. In order to inactivate the enzyme and purify the hydrogel, the subsequent enzymatic calculation of the enzymatic efficiency was facilitated. We also tested the Napkin-PAO hydrogel of different enzymatic time in 16 ppm U-spiked seawater for 160 hours. We conducted a comparative test, immersing the pure hydrogel in the enzymatic hydrolysate for 36 hours, and then weighing the dry weight again, which showed that the cellulase did not work on the pure hydrogel. The blank PAO hydrogel was fabricated the same as the antibacterial Napkin-PAO composite hydrogel, but without napkin paper. The blank non-antibacterial hydrogel was fabricated the same as antibacterial Napkin-PAO composite hydrogel, but without the antibacterial monomer with the quaternary ammonium groups (allyltrimethylammonium chloride).

Test of the Antibacterial Performance

The antibacterial property of the Napkin-PAO composite hydrogels is owing to the quaternary amine groups on the hydrogel network, which has broad-spectrum antibacterial property because the positive ions of them can destroy the cytoderm of the bacteria based on electrostatic force, hydrogen bond and hydrophobic interaction. The antibacterial property of the hydrogel was tested through the plate counting method, and Procedures Refer to national standards, pour sterile solid medium into a Petri dish, and prepare sterile agar plates in a sterile environment. Three kinds of exponential growth bacteria were shifted into a 5 mL fresh LB medium at a ratio of 1.0%. The mass ratio of hydrogel to broth is 1 mg/mL, and cultured at 37 ° for 3 hours in shaker (180 rpm), the cultures of the three bacteria were collected and the bacterial concentration was determined by dilution plate counting, using the formula (1) and calculated via the formula below to calculate the inhibition rate,

$$IR = (C_i - C_a) / C_i \times 100\% \quad (1)$$

where IR is the inhibition rate, C_i , C_a are bacteria number without treating and treated with the antibacterial hydrogel respectively.

Calculation of the Uranium-uptake capacity

We calculated the uranium-uptake amount by the two methods of UV-Vis absorption spectra based on Arsenazo (III) and the ICP-Mass. The uranium concentration in U-spiked water and U-spiked seawater was measured through the UV-Vis absorption spectra based on the Arsenazo (III) which can coordinate with the uranyl ion and shown an intense specific peak at 652 nm, according to the literature.³ A Napkin-PAO composite hydrogel containing 10 mg dry gel was immersed into a 2.0 L U-spiked ultrapure-water or U-spiked seawater solutions and stirred with a table concentrator. The curvilinear regressions of the uranium concentration-absorbance in ultrapure-water (**Figure S1**) and seawater solution (**Figure S2**) respectively have been achieved. The uranium concentration can be detected according to the two standard curves. The concentration of uranium and other micro-ions (U, V, Fe, Cu, Ni, Zn, etc.) in the natural seawater was tested by ICP-Mass through calculating the change of the concentration before and after adsorption.

The uranium adsorption mass can be calculated based on the formula (2):

$$W_U = (C_o - C_t) \times V \quad (2)$$

Where W_U (mg) is the uranium adsorption mass of the hydrogel, C_o (mg/L) and C_t (mg/L) are the uranium concentration of the U-spiked aqueous solution at different time respectively, V (mL) is the volume of the U-spiked solution.

The uranium uptake capacity of Napkin-PAO composite hydrogel can be calculated according to the formula (3):

$$Q_{Hydrogel} = W_U / W_{dry\ gel} \quad (3)$$

Where Q_{Hydrogel} (mg/g) is the uranium uptake capacity of the Napkin-PAO composite hydrogel, W_U (mg) and $W_{\text{dry gel}}$ (g) are the uranium adsorption mass of the dry hydrogel and the mass of Napkin-PAO composite hydrogel respectively.

The uranium adsorption capacity of the PAOs can be calculated via the formula (4):

$$Q_{\text{PAO}} = W_U / W_{\text{PAO}} \quad (4)$$

Where Q_{PAO} (mg/g) is the uranium adsorption capacity of the PAO in the Napkin-PAO composite hydrogel, W_U (mg) and W_{PAO} (mg) are the uranium adsorption mass and the PAO respectively.

Test of the uranium adsorption selectivity of the hydrogel

The metal element adsorption selectivity of the CP-PAO hydrogel was tested within a simulated seawater environment. Natural seawater was selected as the substrate to configure the test solution, and the concentration of V, Fe, Cu, Zn, Ni, and U elements was expanded as 100 times as the original concentration, and the concentrations of other metal elements were not changed.³² We placed 2 mg P-PAO hydrogel into 500 mL test solution, and the adsorbent was removed after adsorbing for 24 hours. After the hydrogel adsorbent is subjected to a nitration treatment, the amount of each adsorbed metal elements was detected by an ICP-MS.

Method of the Uranium Desorption Performance

According to the reported literature,⁴ 11.7 ml 30 % H_2O_2 aqueous solution and 106 g Na_2CO_3 were dissolved ultrapure water to prepare the 1000 mL elution solution. The U-uptake Napkin-PAO composite hydrogel with 10 mg dry gel was immersed in the eluent (200 mL). After stirring for 10 min, the adsorbed uranium in the hydrogel can be desorbed. We can regenerate the hydrogel membrane through immersing it in 500 mL pure water and changing the water several times until the pH = 7. The regenerated Napkin-PAO composite hydrogel was utilized for the next adsorption-desorption cycle.

Method of the Uranium Extraction from the Natural Seawater

The Napkin-PAO composite hydrogel can be fixed between the two nano sponges respectively with a U-adsorption system and extract uranium (**Figure S17a**) in a continuous flowing-through natural seawater. 12 pieces of the Napkin-PAO composite hydrogel was placed in the 12 independent beds, respectively. Each piece of the Napkin-PAO composite hydrogel has 3.0 mg of dry gel (The hydrogel membrane was dried enough for 24 h by a vacuum lyophilizer and then was cut into 3.0 mg pieces.). mass of the seawater is 1.0 T and the flowing speed through the beds were controlled at 1.0 ± 0.1 L/min. All of samples taken from natural seawater were subjected to nitration treatment, and the amount of uranium and vanadium elements was measured by ICP-MS.

Data analysis

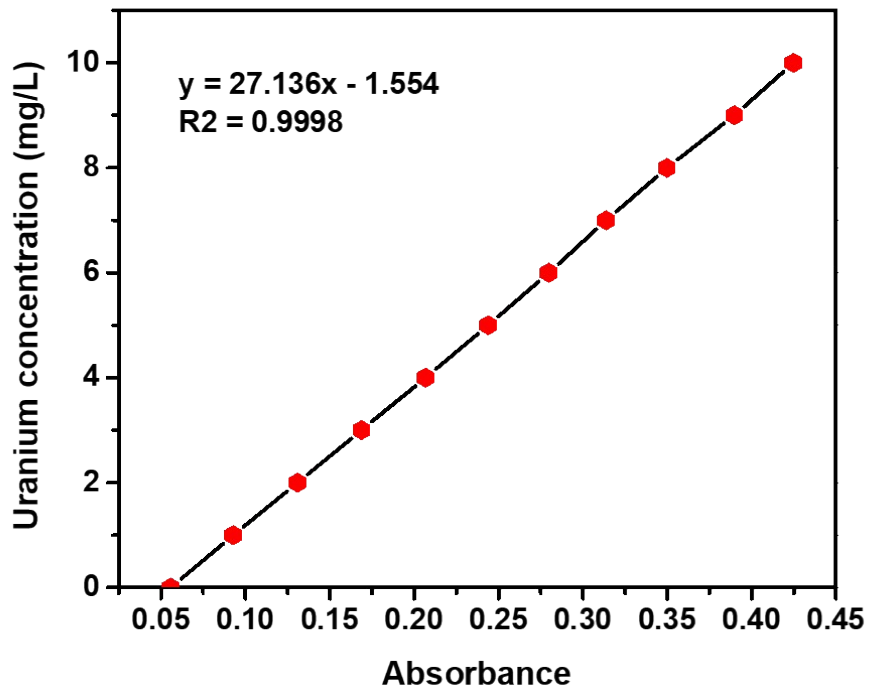


Figure S1 The curvilinear regression of uranium concentration-absorbance in uranium-spiked ultrapure water.

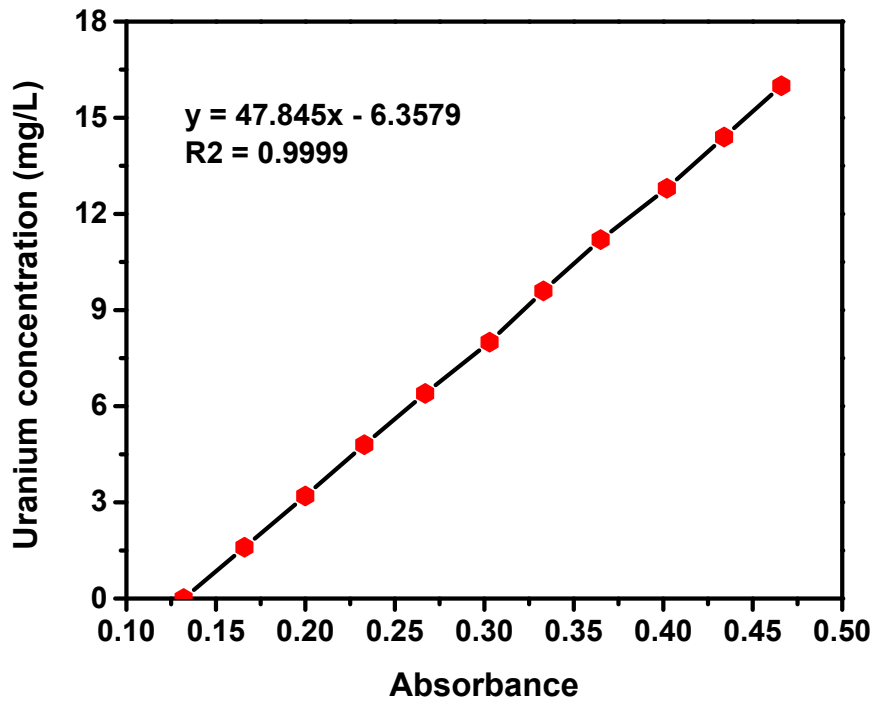


Figure S2 The curvilinear regression of uranium concentration-absorbance in uranium-spiked natural seawater.

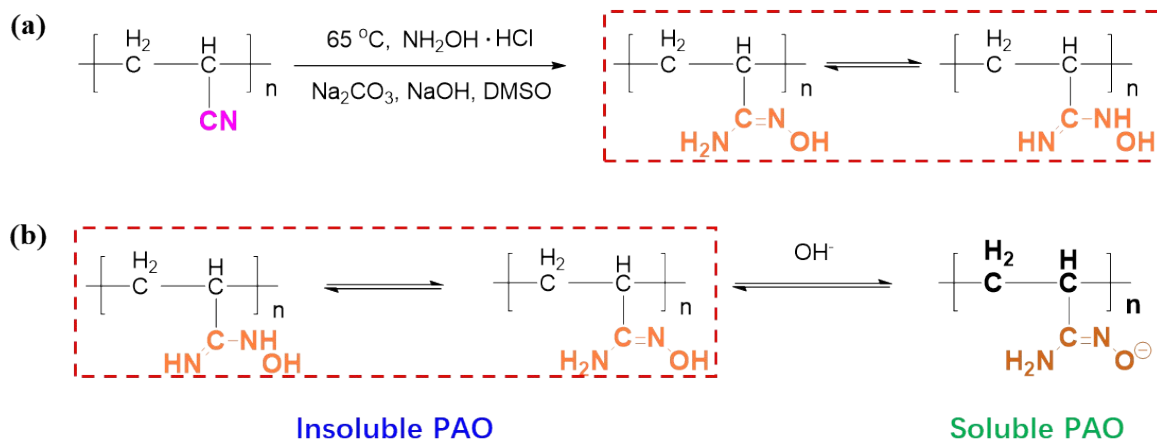


Figure S3 (a) Synthesis of neutral PAO; (b) Transformation from water-insoluble PAO to water-soluble PAO containing negative charges under alkaline condition.

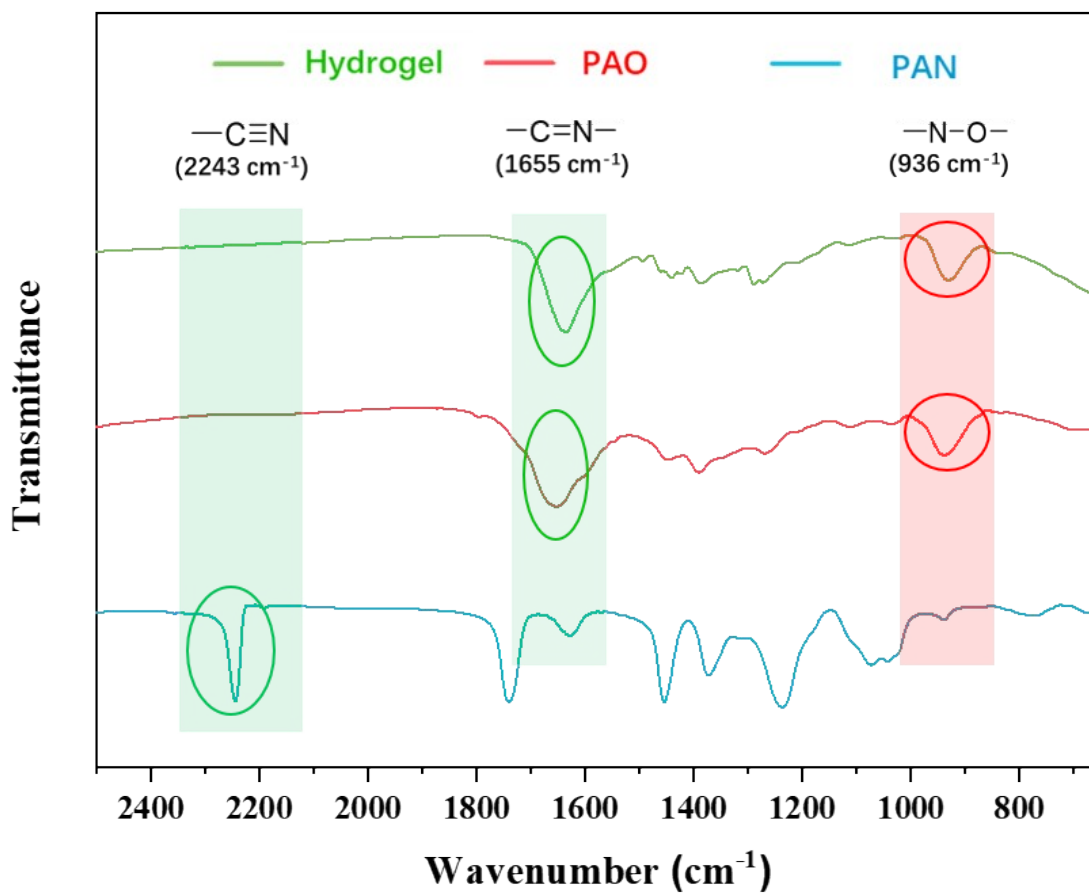


Figure S4 The FT-IR spectra of PAN, PAO and Napkin-PAO hydrogel.

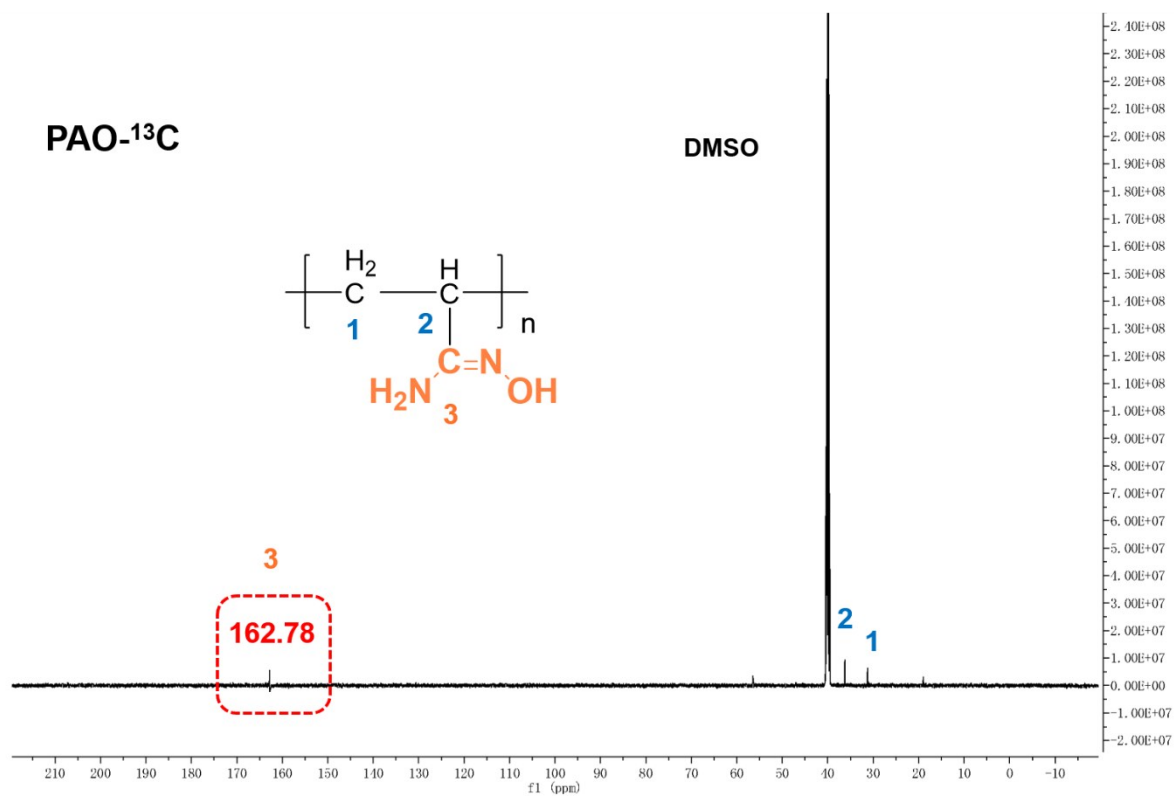
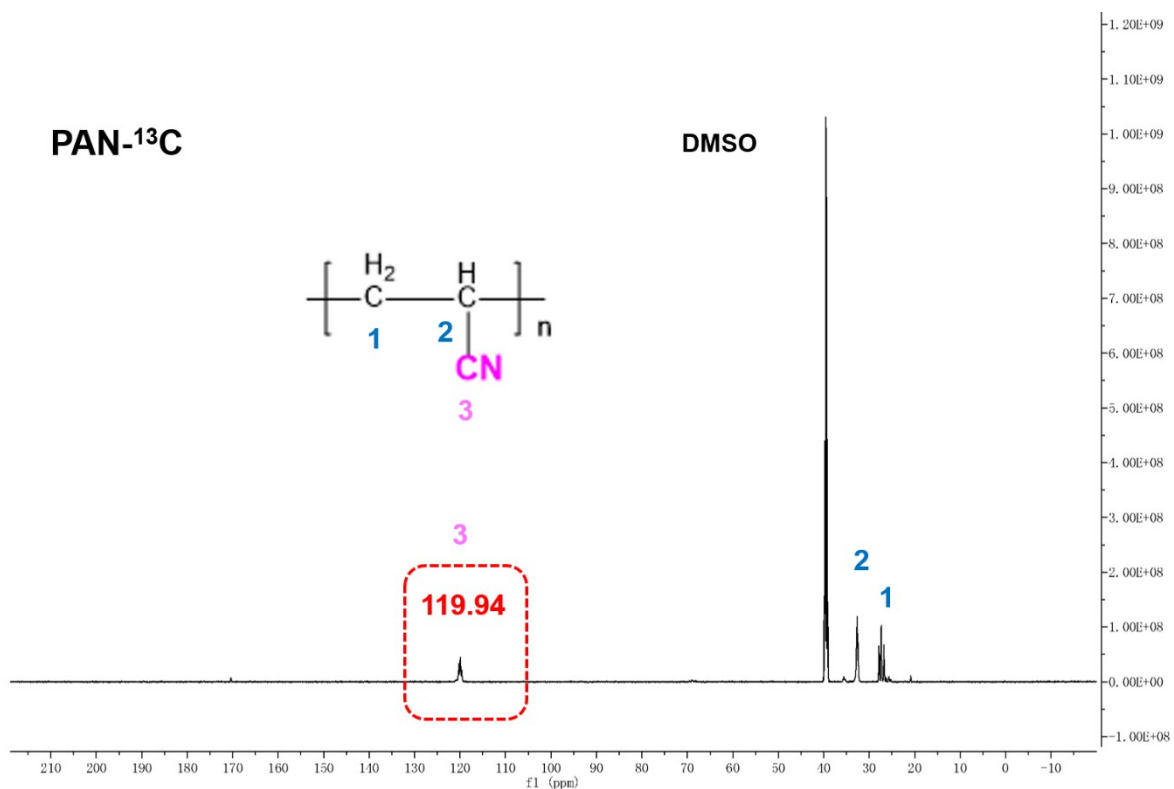


Figure S5 The ¹³C-NMR spectra of (a) PAN and (b) PAO in DMSO-D₆, respectively.

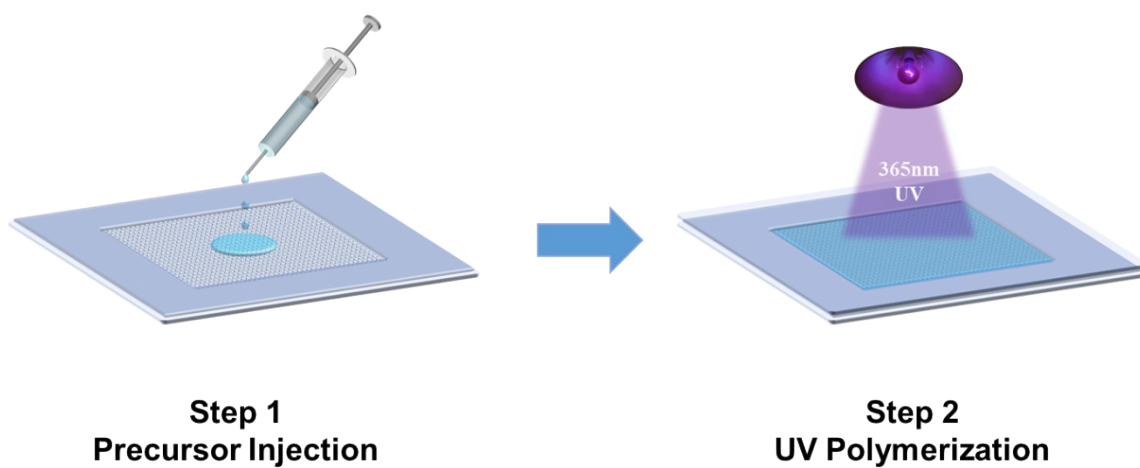


Figure S6 Fabricating process of the primary Napkin-PAO composite hydrogel.

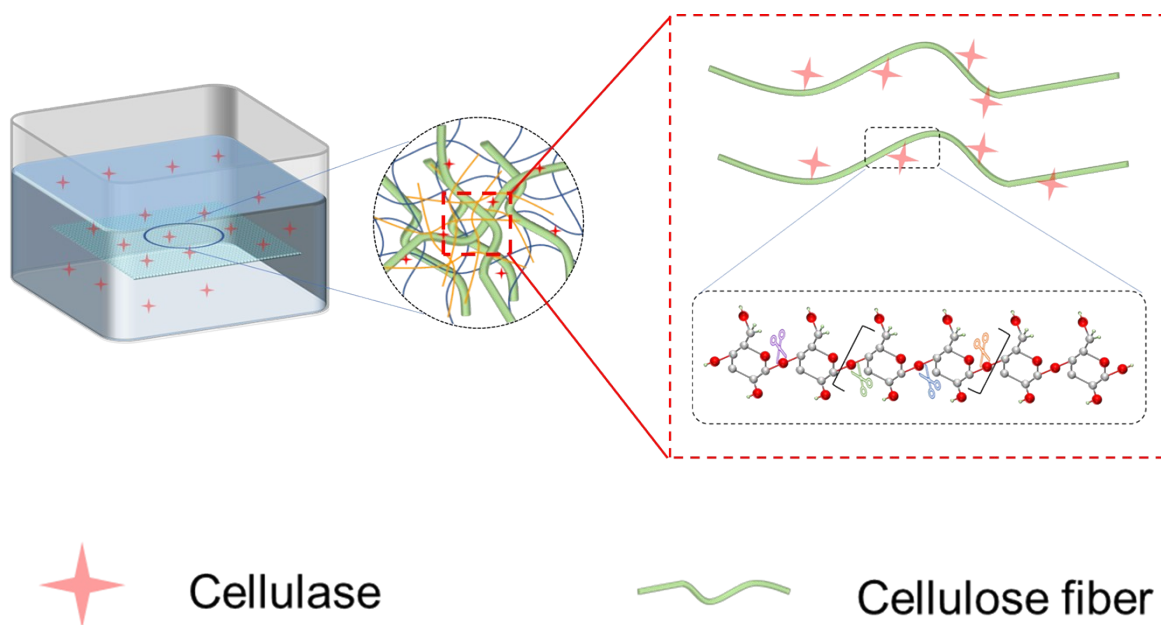


Figure S7 Cellulase enzymatic hydrolysis of the cellulose fiber.

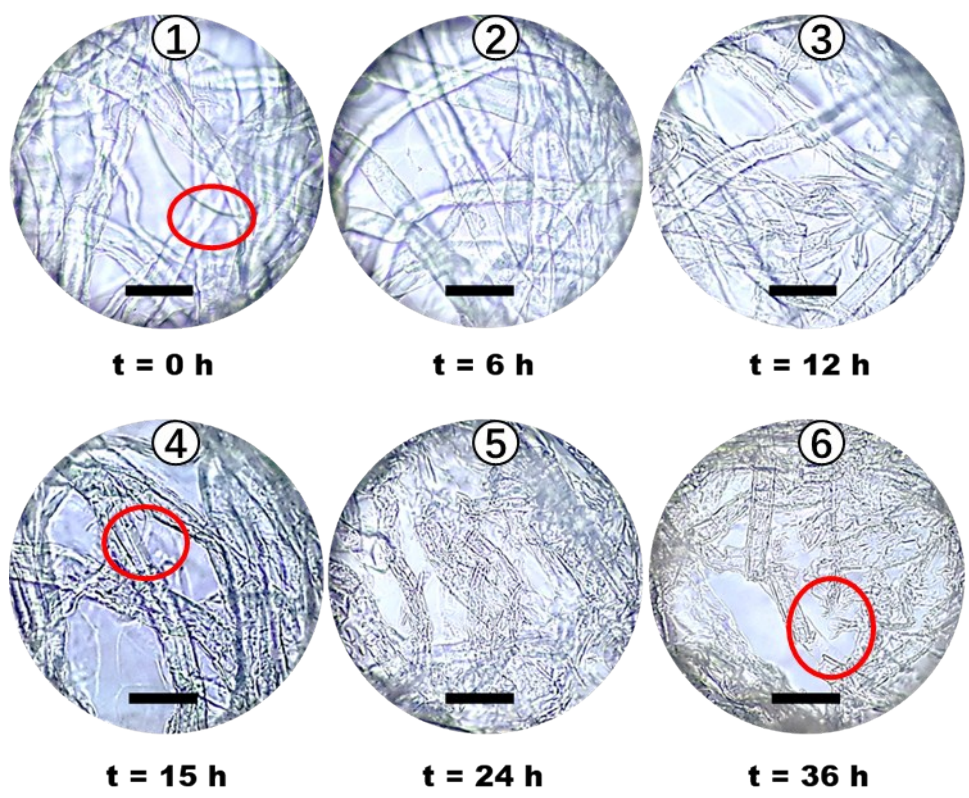


Figure S8 Microscopic photos of composite hydrogel with different hydrolysis time.

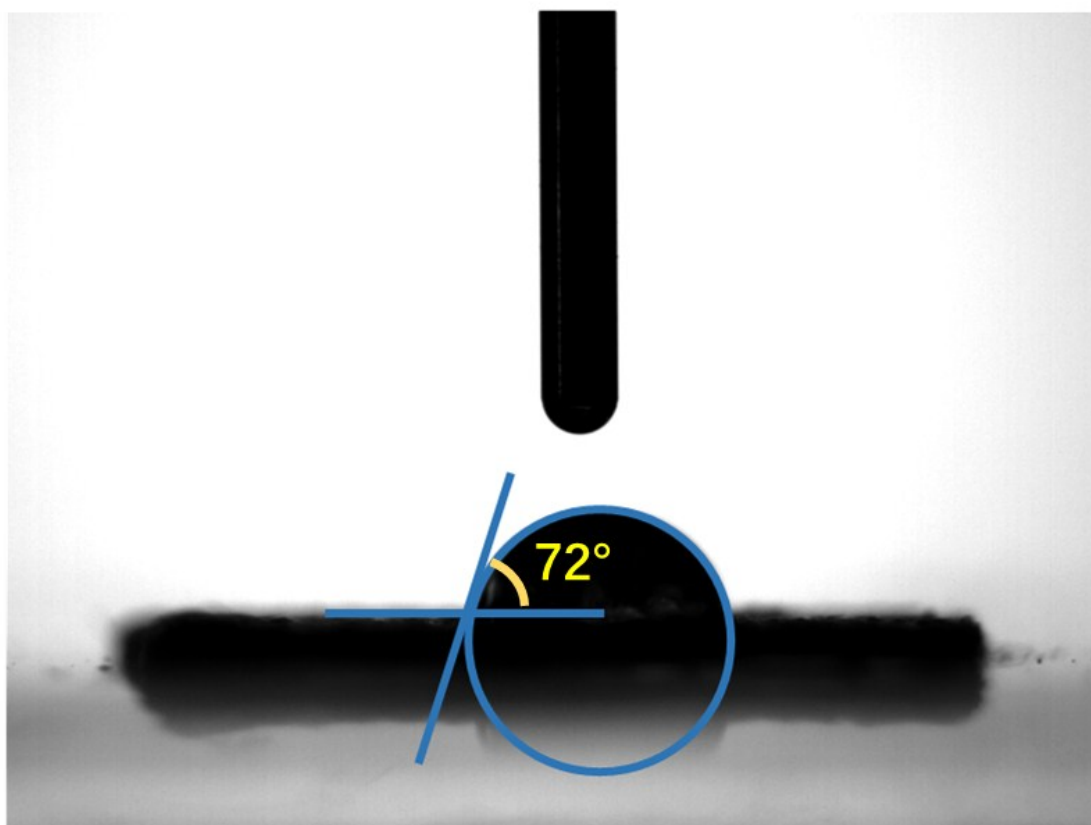


Figure S9 Illustration to detect the contact angle of the (a) PAO and (b) the Napkin-PAO composite hydrogel.

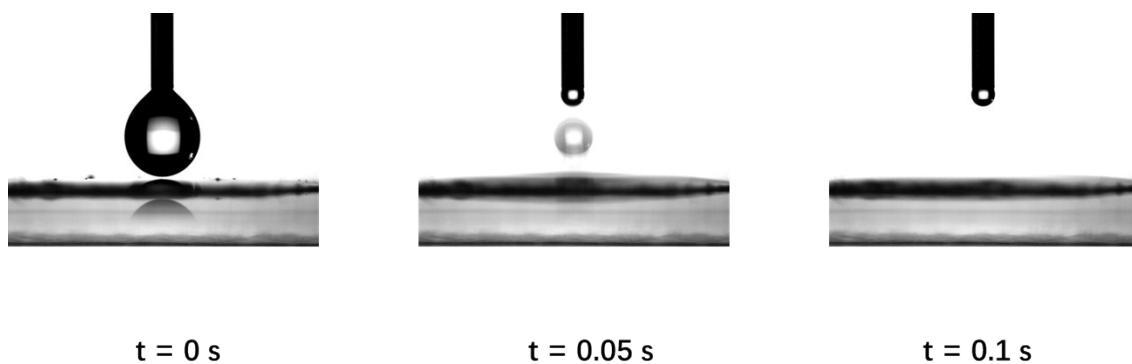


Figure S10 The contact angle of the cellulose-based napkin paper.

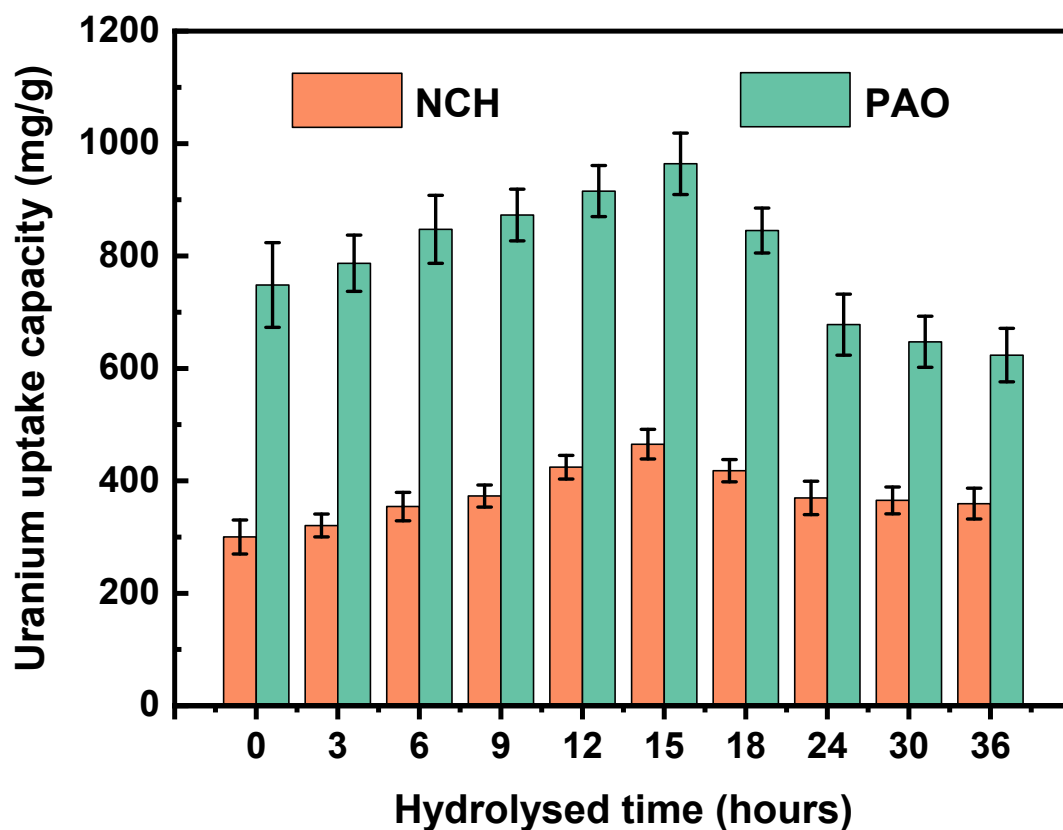


Figure S11 Uranium uptake capacity of composite hydrogel with different hydrolysis time in 16 ppm U-spiked filtered seawater.

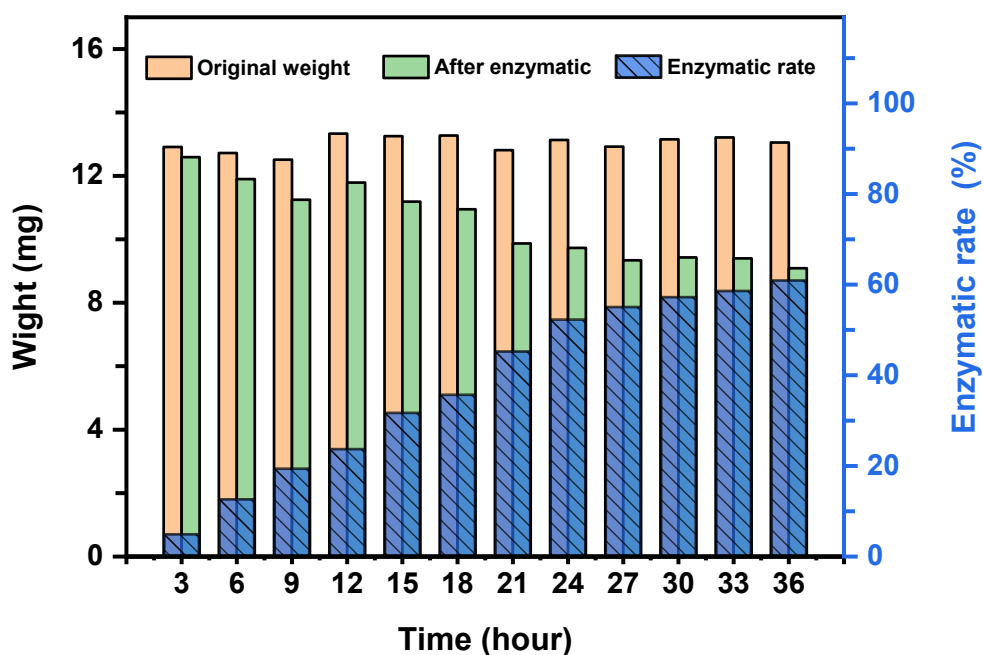


Figure S12 Hydrogel weight and enzymatic hydrolysis rate during enzymatic hydrolysis.

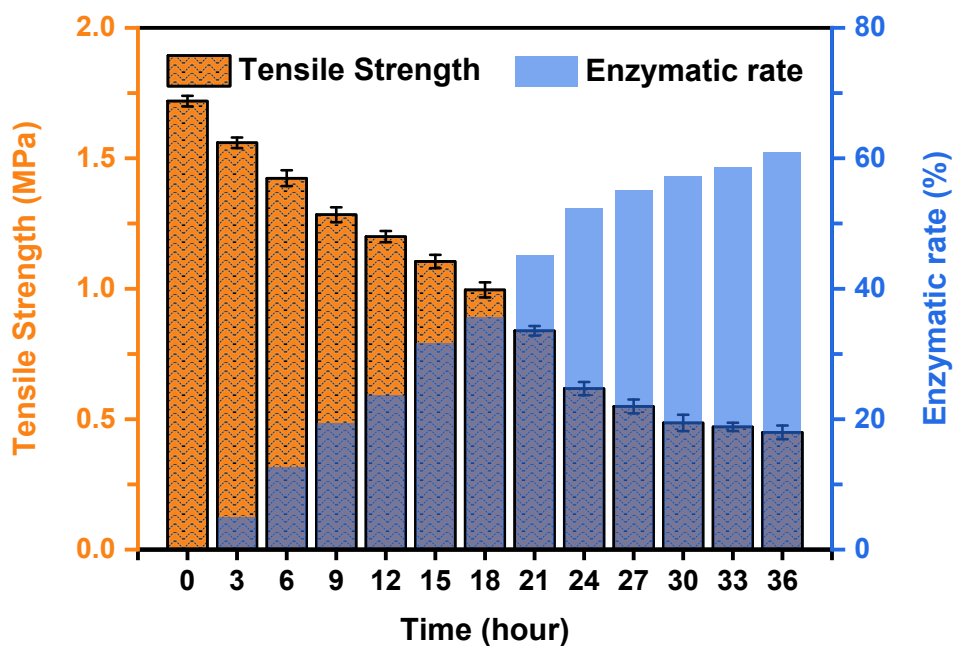


Figure S13 The tensile strengths of composite hydrogels with different enzymatic hydrolysis rate.

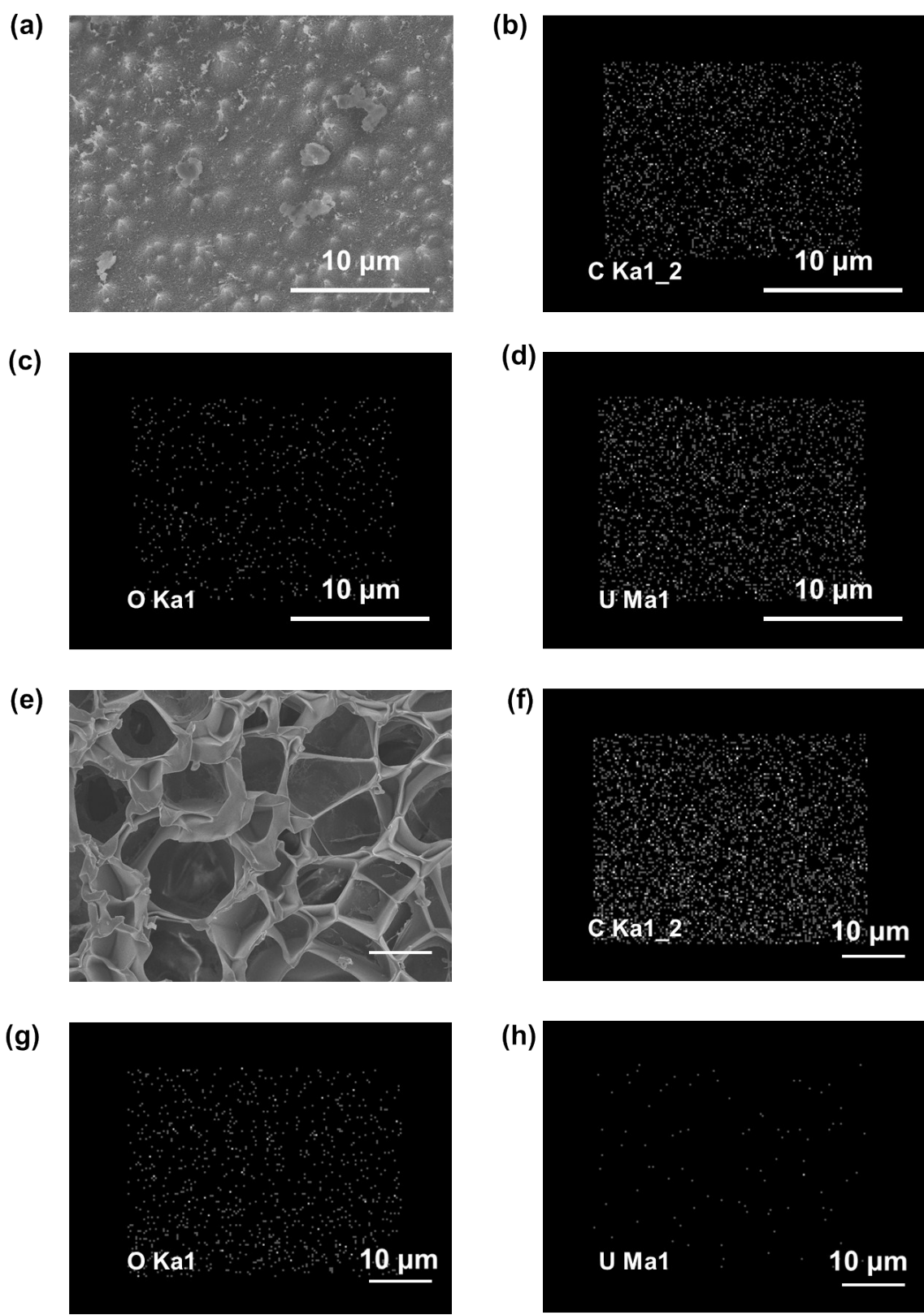


Figure S14 Comparison of the C, O, U EDS mappings between the (a-f) U-uptake hydrogel and the (e-f) original Napkin-PAO composite hydrogel.

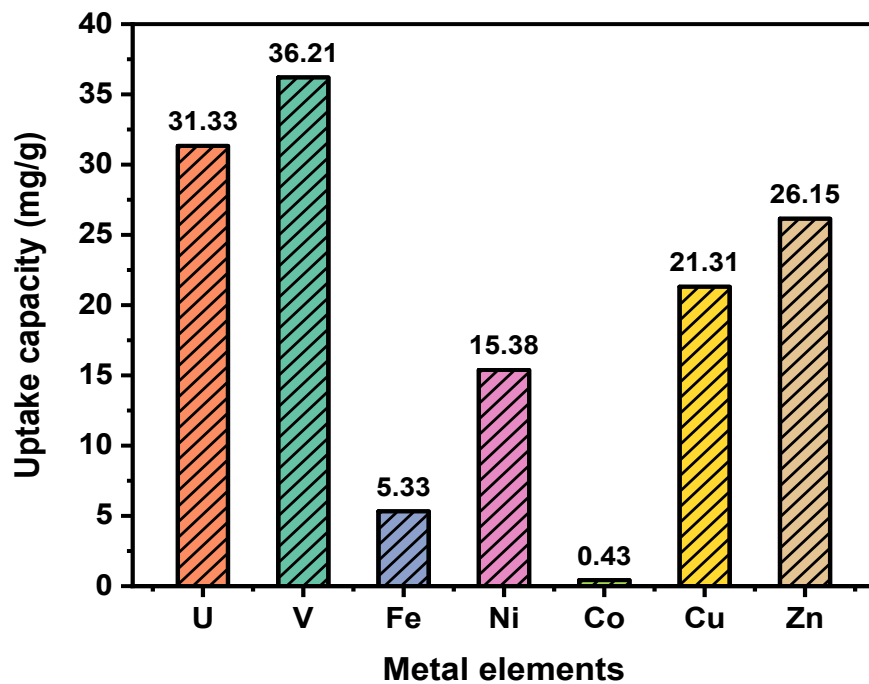


Figure S15 Adsorption selectivity of the CP-PAO hydrogel for uranyl ions in simulated seawater (U, V, Fe, Ni, Co, Cu and Zn are 100 times more concentrated than in natural seawater; Na, Ca, Mg and K are at the same concentration as in natural seawater).

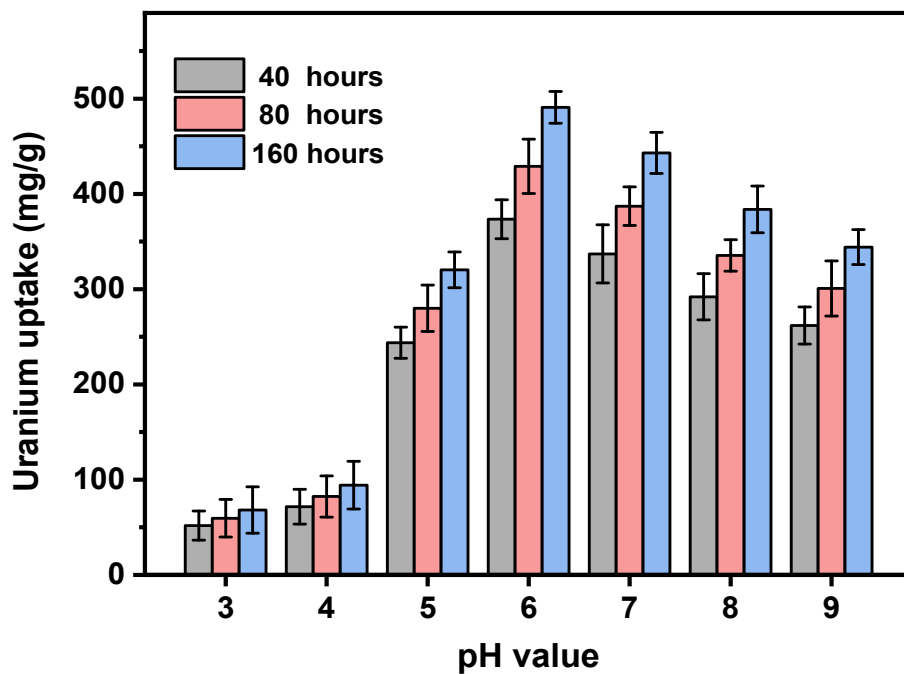


Figure S16 pH dependence of the CP-PAO hydrogel for uranium adsorption in 8 ppm U-spiked pure water.

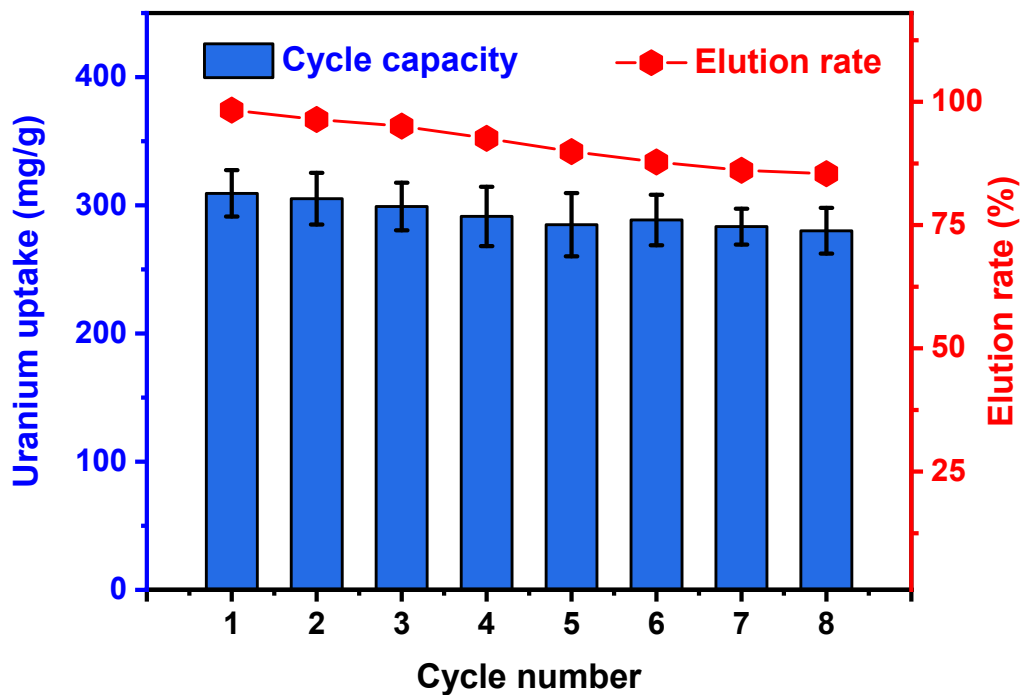


Figure S17 The uranium adsorption capacities (blue columns) and recovery rates of elution (red points) over 8 adsorption-desorption cycles (elution solution of $1.0 \text{ mol L}^{-1} \text{ Na}_2\text{CO}_3$ and $0.1 \text{ mol L}^{-1} \text{ H}_2\text{O}_2$; the adsorption time was 40 hours and the desorption time was 60 min).

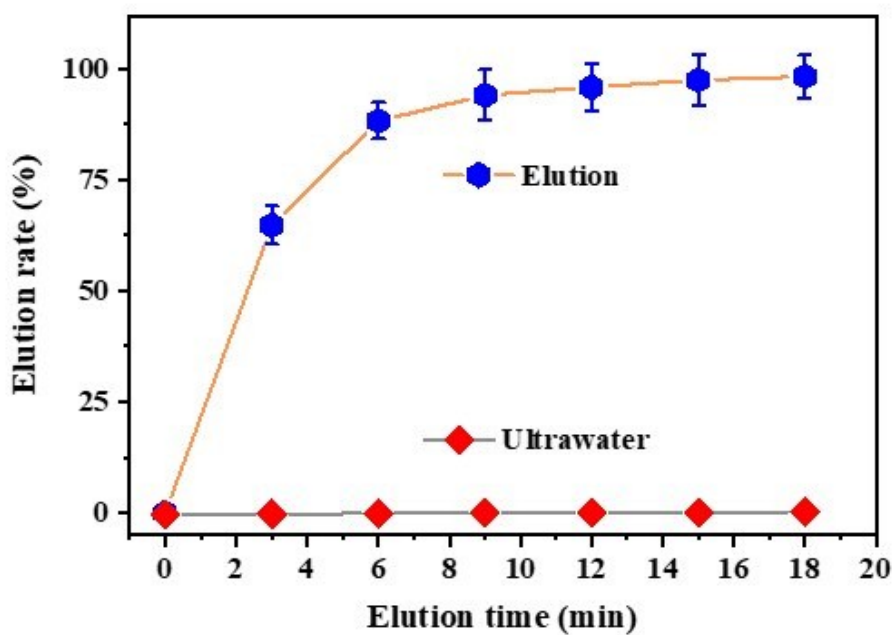


Figure S18 Uranium desorption kinetics of the Napkin-PAO composite hydrogel in the elution solution.

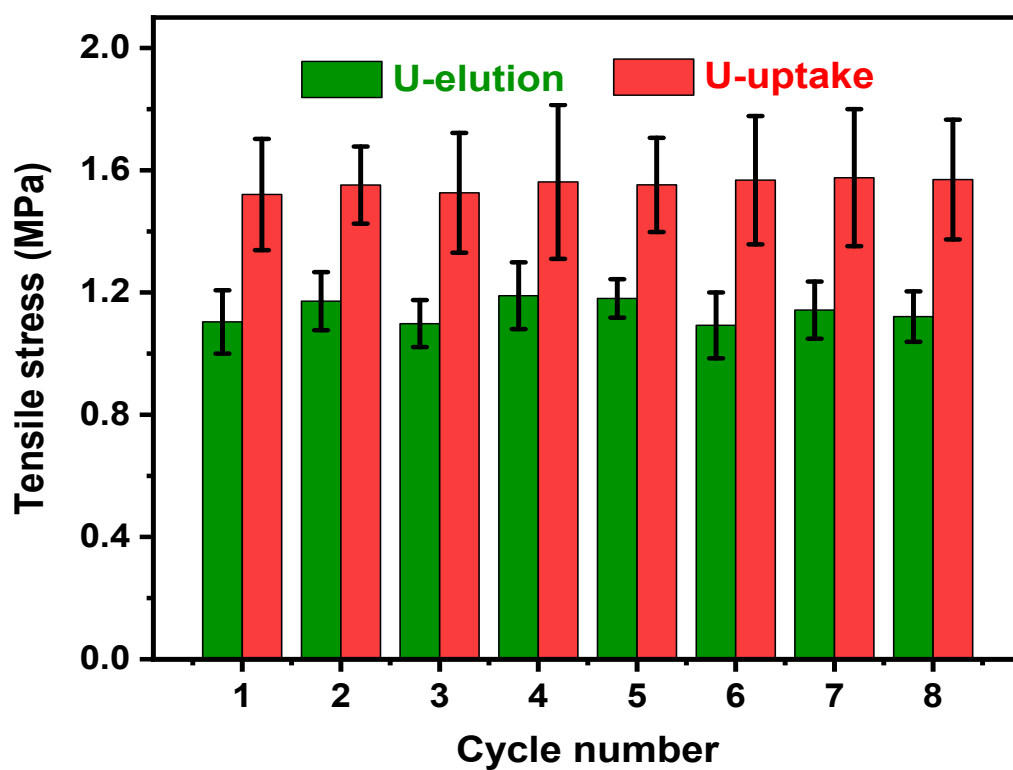


Figure S19 The tensile stress of the antibacterial CP-PAO hydrogel before and after uranium elution over 8 adsorption-desorption cycles.

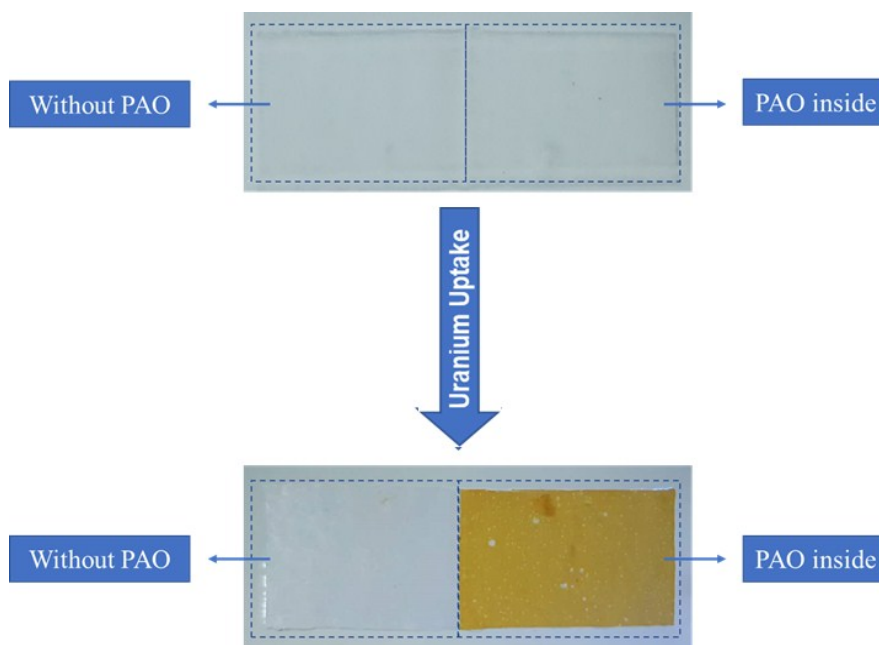


Figure S20 Comparison of uranium extraction between hydrogel substrate and Napkin-PAO composite hydrogel.

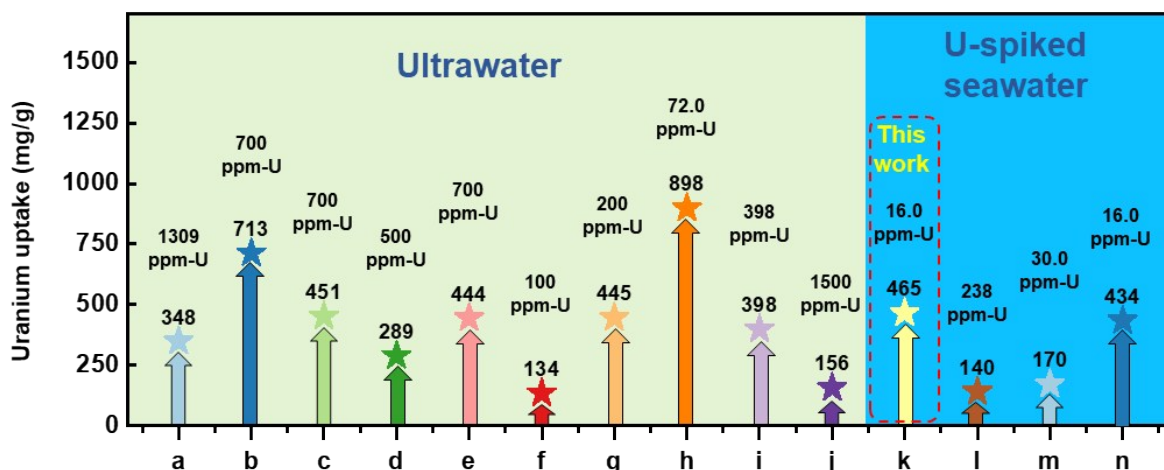


Fig. S21 Comparison of the adsorption capacity of the CP-PAO hydrogel to the hydrogel-based and membrane-based adsorbents in U-spiked water and simulated seawater (The sample k is this hydrogel, the other adsorption capacities of b-j, l-n samples were cited from published papers).^{3,6-17}

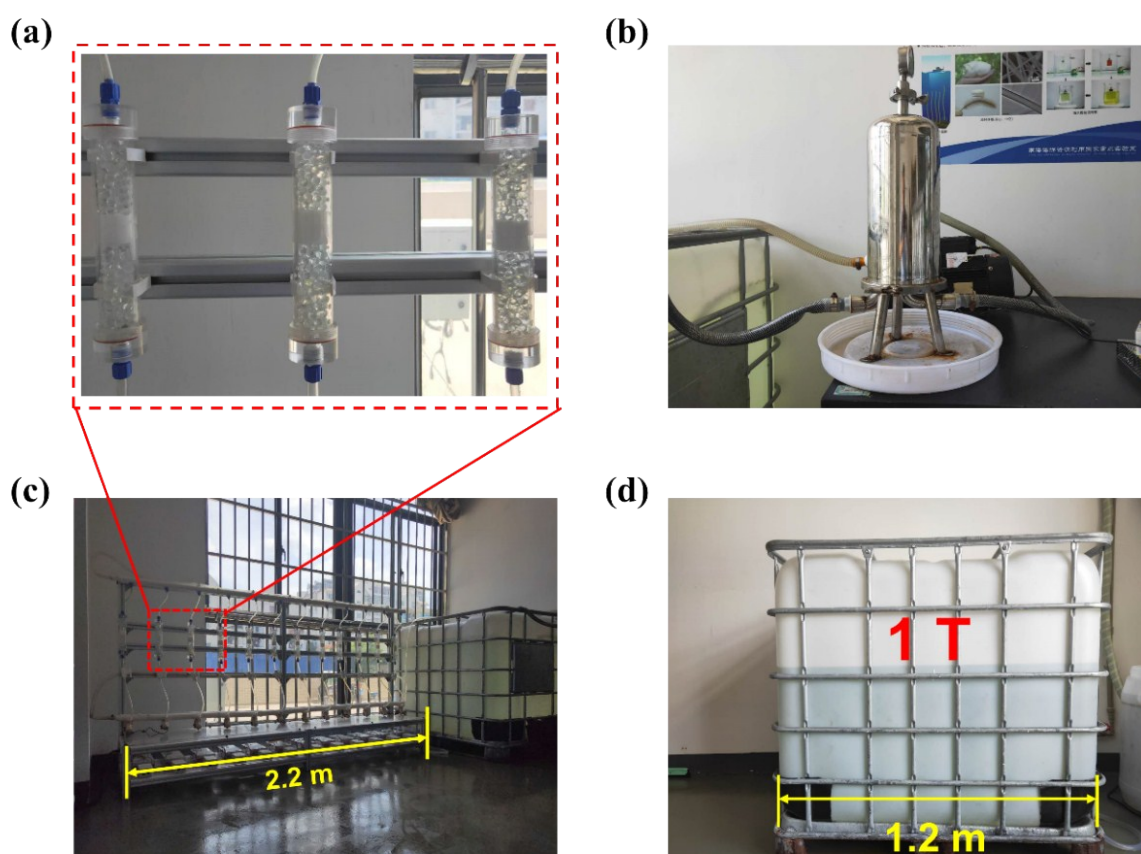


Figure S22 The seawater test system. (a) Plexiglass filter column. (b) Microfiltration membrane pump. (c) Seawater circulation device (including 12 filter columns). (d) Seawater storage vessel (1 ton)

Table S1 Concentration of U(VI) and co-existing metal ions in seawater and 100× seawater. ⁵**Table S1** Concentration of U(VI) and co-existing metal ions in seawater and 100× seawater. ⁵

| Element | Con. In natural SW/ppb | Con. In 100× SW (calculated)/ppb | Ions |
|---------|------------------------|----------------------------------|------------------|
| U | 3.3 | 330 | U(VI) |
| V | 1.5-2.5 | 200 | V(V) |
| Fe | 1.0-2.0 | 150 | Fe ³⁺ |
| Co | 0.05 | 5.0 | Co ²⁺ |
| Ni | 1 | 100 | Ni ²⁺ |
| Cu | 0.6 | 60 | Cu ²⁺ |
| Zn | 4.0 | 400 | Zn ²⁺ |

Table S2 Swelling ratio (SR) and water absorptivity (WA) of hydrogel (Enzymatic hydrolysis time is 15 hours).

| Sample | SR ^a (%) | WA ^b (%) |
|------------------------------|---------------------|---------------------|
| Hydrogel (in 0.15 M NaOH) | 1482 ± 57 | 1382 ± 57 |
| Hydrogel (in water) | 954 ± 33 | 854 ± 33 |
| Hydrogel (in seawater) | 633 ± 41 | 533 ± 41 |

$$\text{a: SR} = [m_{\text{hydrogel}}/m_{\text{dry gel}}] \times 100\%$$
$$\text{b: WA} = [m_{\text{hydrogel}} - m_{\text{dry gel}}] / m_{\text{dry gel}} \times 100\%$$

Table S3. Mechanical properties of hydrogel (Enzymatic hydrolysis time is 15 hours) and adsorption-desorption cycled hydrogels.

| Sample ^a | Strength at break (MPa) | Yang's modulus (MPa) | Elongation at break (%) |
|-------------------------|-------------------------|----------------------|-------------------------|
| Original hydrogel | 1.1032 ±0.0322 | 0.9142 ±0.0182 | 12.0 ± 0.51 |
| Hydrogel after 1 cycle | 1.1718 ±0.0266 | 0.9282 ±0.0336 | 12.6 ± 0.67 |
| Hydrogel after 2 cycles | 1.099 ±0.049 | 0.847 ±0.0266 | 12.9 ± 0.72 |
| Hydrogel after 3 cycles | 1.19 ±0.0378 | 1.0318 ±0.0294 | 11.5 ± 0.43 |
| Hydrogel after 4 cycles | 1.1802 ±0.0238 | 0.875 ±0.0406 | 13.5 ± 0.55 |
| Hydrogel after 5 cycles | 1.0934 ±0.0294 | 0.9282 ±0.0308 | 11.7 ± 0.64 |
| Hydrogel after 6 cycles | 1.1424 ±0.0462 | 0.9044 ±0.0364 | 12.6 ± 0.48 |
| Hydrogel after 7 cycles | 1.1214 ±0.035 | 0.9058 ±0.0294 | 12.4 ± 0.59 |

a: All the hydrogel membrane samples with a dumbbell shape (length: 50 mm, width: 10 mm) were prepared for the tensile testing. All the tests were measured at a constant rate of 50 mm/min.

Supporting Movies

Movie S1. Preparation process of the Napkin-PAO composite hydrogel.

Movie S2. The Napkin-PAO composite hydrogel mechanical strength display.

Movie S3. U-adsorption process of the Napkin-PAO composite hydrogel in 100 ppm U-spiked water.

Movie S4. U-desorption process of the U-uptake Napkin-PAO composite hydrogel in elution solution.

References

- 1 H.-B. Pan, L.-J. Kuo, C. M. Wai, N. Miyamoto, R. Joshi, J. R. Wood, J. E. Strivens, C. J. Janke, Y. Oyola, S. Das, R. T. Mayes and G. A. Gill, *Ind. Eng. Chem. Res.*, 2016, **55**, 4313-4320.
- 2 S. O. Kang, S. Vukovic, R. Custelcean and B. P. Hay, *Ind. Eng. Chem. Res.*, 2012, **51**, 6619-6624.
- 3 C. Ma, J. Gao, D. Wang, Y. Yuan, J. Wen, B. Yan, S. Zhao, X. Zhao, Y. Sun, X. Wang and N. Wang, *Adv. Sci.*, 2019, **6**, 1900085.
- 4 H.-B. Pan, W. Liao, C. M. Wai, Y. Oyola, C. J. Janke, G. Tian and L. Rao, *Dalton Trans.*, 2014, **43**, 10713-10718.
- 5 D. Wang, J. Song, J. Wen, Y. Yuan, Z. Liu, S. Lin, H. Wang, H. Wang, S. Zhao, X. Zhao, M. Fang, M. Lei, B. Li, N. Wang, X. Wang and H. Wu, *Adv. Energy Mater.*, 2018, **8**, 1802607.
- 6 F. Xiao, Y. Sun, W. Du, W. Shi, Y. Wu, S. Liao, Z. Wu and R. Yu, *Adv. Funct. Mater.*, 2017, **27**, 1702147.
- 7 F. Wang, H. Li, Q. Liu, Z. Li, R. Li, H. Zhang, L. Liu, G. A. Emelchenko and J. Wang, *Sci. Rep.*, 2016, **6**, 19367.
- 8 X. Wang, Q. Liu, J. Liu, R. Chen, H. Zhang, R. Li, Z. Li and J. Wang, *Appl. Surf. Sci.*, 2017, **426**, 1063-1074.
- 9 R. H. Moghaddam, S. Dadfarnia, A. M. H. Shabani and M. Tavakol, *Carbohydr. Polym.*, 2019, **206**, 352-361.
- 10 C. Wei, M. Yang, Y. Guo, W. Xu, J. Gu, M. Ou and X. Xu, *J. Radioanal. Nucl. Chem.*, 2018, **315**, 211-221.
- 11 J. He, J. Jin, Z. Wang, H. Yin, C. Wei and X. Xu, *J. Radioanal. Nucl. Chem.*, 2019, **317**, 1299-1309.
- 12 J. He, F. Sun, F. Han, J. Gu, ou Minrui, W. Xu and X. Xu, *RSC Adv.*, 2018, **8**, 12684-12691.
- 13 S. Su, R. Chen, Q. Liu, J. Liu, H. Zhang, R. Li, M. Zhang, P. Liu and J. Wang, *Chem. Eng. J.*, 2018, **345**, 526-535.
- 14 Y.-R. He, S.-C. Li, X.-L. Li, Y. Yang, A.-M. Tang, L. Du, Z.-Y. Tan, D. Zhang and H.-B. Chen, *Chem. Eng. J.*, 2018, **338**, 333-340.
- 15 X. Yi, Z. Xu, Y. Liu, X. Guo, M. Ou and X. Xu, *RSC Adv.*, 2017, **7**, 6278-6287.
- 16 P. Akkas and O. Güven, *J. Appl. Polym. Sci.*, 2000, **78**, 284-289.
- 17 L. Zhou, H. Zou, Y. Wang, Z. Liu, Z. Le, G. Huang, T. Luo and A. A. Adesina, *J. Radioanal. Nucl. Chem.*, 2017, **311**, 779-787.